EMBO reports

TRANSPARENT PROCESS

scientific report

Piezo1-dependent stretch-activated channels are inhibited by Polycystin-2 in renal tubular epithelial cells

Rémi Peyronnet[1], Joana R Martins[1]*, Fabrice Duprat[1], Sophie Demolombe[1], Malika Arhatte[1], Martine Jodar[1], Michel Tauc[2], Christophe Duranton[2], Marc Paulais[3], Jacques Teulon[3], Eric Honoré[1†+] & Amanda Patel[1†]*

[1]Institut de Pharmacologie Moléculaire et Cellulaire, LabEx ICST, UMR 7275 CNRS, Université de Nice Sophia Antipolis, Valbonne, France, [2]CNRS-FRE 472, Laboratoire de Physiomédecine Moléculaire, Université de Nice Sophia Antipolis, Nice, France, and [3]UPMC Université Paris 06, UMR 872 CNRS, Laboratoire de Génomique, Physiologie et Physiopathologie Rénales, Paris, France

Mechanical forces associated with fluid flow and/or circumferential stretch are sensed by renal epithelial cells and contribute to both adaptive or disease states. Non-selective stretch-activated ion channels (SACs), characterized by a lack of inactivation and a remarkably slow deactivation, are active at the basolateral side of renal proximal convoluted tubules. Knockdown of Piezo1 strongly reduces SAC activity in proximal convoluted tubule epithelial cells. Similarly, overexpression of Polycystin-2 (PC2) or, to a greater extent its pathogenic mutant PC2-740X, impairs native SACs. Moreover, PC2 inhibits exogenous Piezo1 SAC activity. PC2 coimmunoprecipitates with Piezo1 and deletion of its N-terminal domain prevents both this interaction and inhibition of SAC activity. These findings indicate that renal SACs depend on Piezo1, but are critically conditioned by PC2.

Keywords: Fam38A; kidney; Piezo1; PKD; mechanotransduction; TRP channels

EMBO *reports* (2013) **14,** 1143–1148. doi:10.1038/embor.2013.170

INTRODUCTION

Mechanotransduction concerns the cellular responses to a variety of mechanical stimuli [1–7]. Specialized mechano-sensitive cells, such as hair cells in the inner ear or dorsal root ganglion touch receptors, are equipped with highly sensitive transduction channel complexes. Nevertheless, even non-specialized cells respond to mechanical stress by activating a panel of mechanosensors, among them stretch-activated ion channels (SACs) [8]. In the kidney, important progress has recently been made in the understanding of flow sensing by tubular epithelial cells [9,10]. Bending of the primary cilium at the apical side of tubular cells induced by the flow of intraluminal urine activates the ciliary polycystin complex (Polycystin-1, PC1, and Polycystin-2, PC2, which are mutated in autosomal dominant polycystic kidney disease), resulting in a calcium influx through the transient receptor potential (TRP) channel PC2 (for reviews: [11–14]). However, kidney epithelial cells also respond to changes in intraluminal pressure [11,13]. Normal pressure at rest within the renal pelvis and ureter is in the range of 0–10 mm Hg. However, peristaltic pressures generated by rhythmic papillary contractions required for the transport of urine vary between 15 and 45 mm Hg [11]. When a renal tubule is subjected to intraluminal pressure, both apical and basolateral membranes are stretched [15]. This physiological transient elevation in pressure is transmitted back to the tubular lumen and leads to repetitive tubular distension and cell stretching. Intraluminal pressure can also be dramatically elevated in kidney disease states [11]. Indeed, obstructive uropathy is associated with a major increase in intratubular pressure, in excess of 60 mm Hg, leading to tubular circumferential stretch [16–20]. Stretching as well as compression of renal epithelial cells also occur in polycystic kidney disease (PKD) patients [11]. Abnormal fluid accumulation in renal cysts causes the cyst wall to stretch [21–23]. Moreover, growing cysts compress neighbouring tubules with upstream accumulation of urine leading to increased intratubular pressure. Stretch of epithelial cells has been proposed to impact on cell proliferation, fibrosis, as well as apoptosis [16–20,23,24]. Thus, pressure-induced stretch of tubular epithelial cells is relevant to both physiological and diseased kidney conditions [11].

Recent findings from the Patapoutian laboratory demonstrate that Piezo1 and Piezo2 are essential components of distinct mechanically activated cation channels [25]. Importantly, using bilayer reconstitution experiments, it was further shown that Piezo proteins

[1]Institut de Pharmacologie Moléculaire et Cellulaire, LabEx ICST, UMR 7275 CNRS, Université de Nice Sophia Antipolis, Valbonne, France
[2]CNRS-FRE 472, Laboratoire de Physiomédecine Moléculaire, Université de Nice Sophia Antipolis, Nice, France
[3]UPMC Université Paris 06, UMR 872 CNRS, Laboratoire de Génomique, Physiologie et Physiopathologie Rénales, Paris, France
*These authors contributed equally to this work.
†These authors contributed equally to this work.
+Corresponding author. Tel: +33 493 957745; Fax: +33 493 957704; E-mail: honore@ipmc.cnrs.fr

Received 6 May 2013; revised 7 October 2013; accepted 7 October 2013; published online 25 October 2013

are pore-forming subunits [26]. The function of *Drosophila* Piezo has recently been shown in mechanical nociception, in line with the role of mouse Piezo2 in pain-sensitive dorsal root ganglion neurons [25,27]. Moreover, gain-of-function mutations in the mechanically activated ion channel Piezo 2 cause a subtype of distal arthrogryposis [28]. In addition, gain-of-function mutations in Piezo1 are associated with xerocytosis, an autosomal dominant haemolytic anaemia characterized by dehydration of erythrocytes [29–31]. However, very little is now known about the possible functional role of Piezo1 in other cell types, including the kidney.

Here, we report the evidence for non-selective SACs active at the basolateral side of renal tubular epithelial cells and characterized by a lack of inactivation and a very slow deactivation. Furthermore, we demonstrate that Piezo1 is required for SAC activity in proximal convoluted tubule (PCT) cells, but its stretch sensitivity is highly regulated by PC2.

RESULTS AND DISCUSSION

Cell-attached patch-clamp recordings were performed on the basolateral side of isolated mouse renal PCTs. SAC activity recorded at a holding potential of −80 mV was elicited by increasing negative pressure at the back of the recording electrode using a fast pressure-clamp system (Fig 1A). Currents were characterized by a fast activation, lack of inactivation and a slow deactivation on termination of the pressure pulse (Fig 1A). The reversal potential of SACs was around 0 mV, indicating a non-selective permeation (Fig 1A). No successful patches could be obtained from the apical side of isolated renal tubules. In cultured immortalized PCT epithelial cells, SACs were similarly non-inactivating with a slow deactivation (Fig 1B). Single-channel conductance of SACs measured in PCT cells was 31.8 ± 0.3 pS ($n = 5$; Fig 1C). SAC activity was inhibited by the addition of ruthenium red (50 μM, $n = 20$) or 5 μM GsMTx-4 (L optical isomer, $n = 13$) to the patch pipette external medium (Fig 1D). In 54% of the active patches ($n = 35$), we also observed stretch-activated K^+ channels, presumably TREK-2 ([24]), at a holding potential of 0 mV and reversing at −80 mV (not shown).

Expression of Piezo1 was detected by quantitative PCR (QPCR) on whole kidney, isolated PCT or immortalized cultured PCT cells, whereas expression of Piezo2 was low or barely detectable in cultured PCT cells (Fig 2A). Transfection of two previously validated short interfering RNAs (siRNAs) [25] into PCT cells, resulted in a Piezo1 knockdown of approximately 70–80% without affecting *Pkd1*, *Pkd2* or other TRP channel subunits expression (supplementary Fig S1 online). SAC activity was strongly reduced in those transfected cells (Fig 2B). These findings indicate that Piezo1 is critically required for SAC activity in PCT cells.

Previously, we showed that SACs in arterial myocytes are modulated by the polycystin PC1/PC2 ratio [32]. Free PC2 (that is, in the absence of PC1) or its overexpression (in the presence of PC1) inhibited SACs in vascular smooth muscle cells [11,32]. We investigated whether PC2 might similarly regulate SAC activity in renal tubular epithelial cells. We overexpressed PC2-WT or the PC2-740X pathogenic mutant (lacking an endoplasmic retention motif and the PC1 interacting coiled-coil domains) in WT PCT cells [24,32–37]. SAC activity was notably reduced, with the stronger inhibition obtained with PC2-740X (Fig 3A–C). Similarly, expression of the pathogenic point mutant PC2D509V induced SAC inhibition in PCT cells (−53% at −50 mm Hg, $n = 23$). Neither

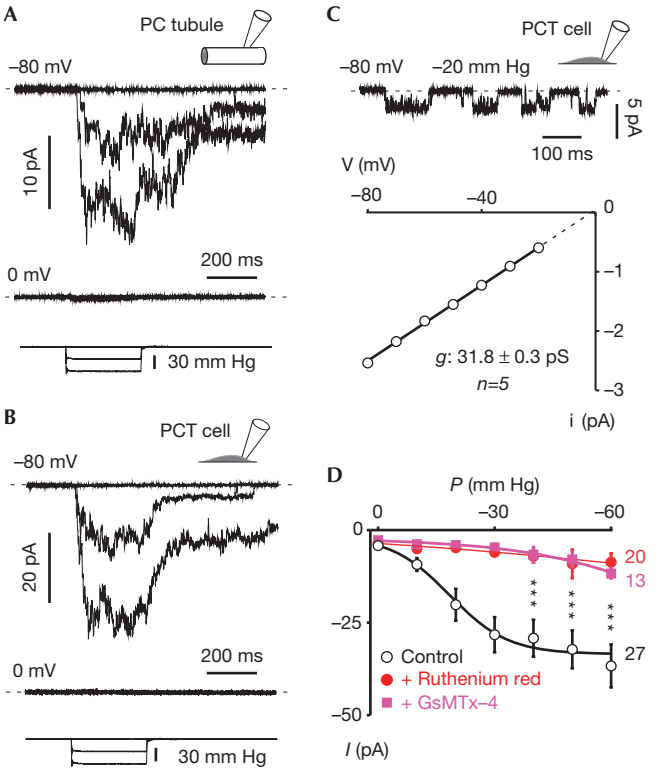

Fig 1 | Native SACs in PCT epithelial cells. (**A**) Top trace: Cell-attached patch-clamp recording of SACs at a holding potential of −80 mV on the basolateral side of a freshly isolated proximal convoluted tubule. Middle trace: same patch at a holding potential of 0 mV. Bottom trace illustrates the pressure pulses. (**B**) Top trace: SAC activity recorded in a cultured isolated wild-type PCT cell at a holding potential of −80 mV. Middle trace: same patch at a holding potential of 0 mV. Bottom trace illustrates the pressure pulses. (**C**) Single channel currents recorded at −80 mV and elicited by a continuous −20 mm Hg pressure stimulation. *I–V* curve of SACs in PCT cells recorded at −20 mm Hg (linear regression). The single channel conductance of SACs in PCT is 31.8 ± 0.3 pS ($n = 5$) and the extrapolated reversal potential around 0 mV. (**D**) Pressure-effect curves in control conditions (black traces), in the presence of 50 μm ruthenium red (red traces) or in the presence of 5 μM GsMTx-4 L optical isomer (magenta traces). GsMTx-4 might act as a gating modifier with partition in the lipid bilayer and shift of the pressure-effect curve to stronger stimuli [40]. PCT, proximal convoluted tubule; SAC, stretch-activated ion channel.

the pressure value required to elicit the opening of 50% of SACs ($P_{0.5}$) nor the slope factor (k) was substantially modified by PC2-740X expression (Fig 3C). The single-channel current amplitude (i) of SACs at −80 mV and the open channel probability (P_o) were not altered in PCT cells expressing PC2-740X, suggesting that the number of active channels (N) was decreased (supplementary Fig S2 online). Of note, Piezo1 mRNA expression in the PCT cells overexpressing PC2-740X was not significantly different from the control cells (supplementary Fig S3 online).

Next, we investigated whether PC2 and its pathogenic mutants might similarly modulate the stretch sensitivity of heterologously expressed Piezo1 (Fig 4). Exogenous Piezo1 currents in PCT cells

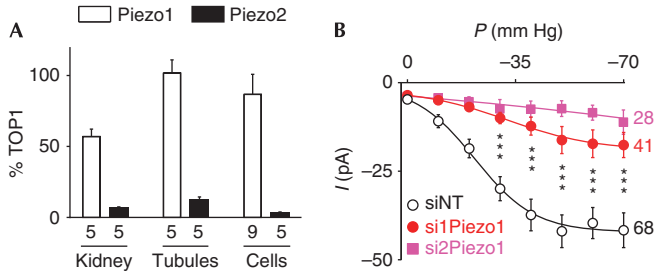

Fig 2 | Endogenous SAC activity in PCT epithelial cells critically depends on Piezo1. (**A**) Quantitative PCR expression of Piezo1 and Piezo2 normalized to Topoisomerase 1 (TOP1) expression in whole kidney, isolated proximal tubules and immortalized PCT cells. (**B**) Pressure-effect curves for mean SAC activity recorded in cultured PCT cells either transfected with a non-targeting siRNA (NT; $P_{0.5} = -21.8 \pm 2.8$ mm Hg, $k = 9.7 \pm 3.4$, $n = 68$) or with two different siRNAs directed against Piezo1 (si1Piezo1; $n = 41$ and si2Piezo1; $n = 28$). PCT, proximal convoluted tubule; SAC, stretch-activated ion channel; siRNA, short interfering RNA.

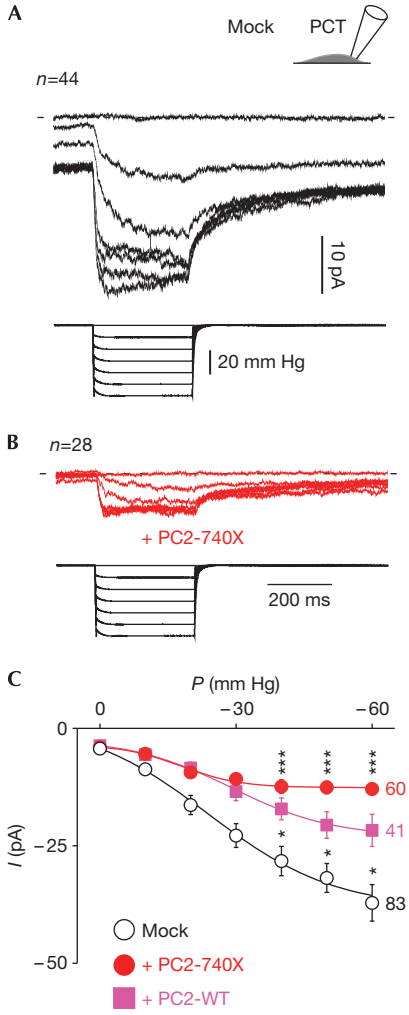

Fig 3 | Endogenous SAC activity in PCT epithelial cells is conditioned by PC2 and PC2-740x. Mean ($n = 44$) cell-attached SAC current (in black) at a holding potential of -80 mV in cultured PCT cells transfected with a mock expression EGFP vector. (**B**) Mean ($n = 28$) cell-attached SAC current (in red) at a holding potential of -80 mV in cultured PCT cells transfected with PC2-740X ires2-EGFP. In **A** and **B**, bottom traces illustrate the pressure pulses. Same scales for **A** and **B**. (**C**) Pressure-effect curve for SAC activity in wild-type PCT cells transfected with either the mock EGFP vector (in black: $P_{0.5} = -16.0 \pm 1.7$ mm Hg, $k = 10.4 \pm 2.4$ or with PC2 ires2-EGFP in magenta: $P_{0.5} = -32.8 \pm 12.8$ mm Hg, $k = 15.8 \pm 10.6$ or with PC2-740X ires2-EGFP in red: $P_{0.5} = -9.6 \pm 1.9$ mm Hg, $k = 7.7 \pm 1.3$). EGFP, enhanced green fluorescent protein; PC2, Polycystin-2; PCT, proximal convoluted tubule; SAC, stretch-activated ion channel.

were significantly higher than native SAC currents (Fig 4A,B and supplementary Fig S4a,b online). In agreement with earlier reports [25,26], the current kinetics of exogenous Piezo1 (digitally subtracted from the mean native SACs current) were characterized by a fast activation, prominent inactivation ($\tau = 49.6 \pm 1.5$ ms, $n = 22$), a rapid deactivation on termination of the pressure pulse ($\tau = 8.2 \pm 0.5$ ms, $n = 22$) and a reversal potential of about 0 mV (supplementary Fig S5 online). When coexpressed with PC2-740X in PCT cells, Piezo1 activity was substantially reduced (Fig 4A,B). Next, we coexpressed Piezo1 together with the PC2-740X mutant in COS-7 kidney fibroblasts (Fig 4C,D and supplementary Fig S4c,d online). Again, exogenous Piezo1 currents in COS-7 cells (digitally subtracted from the mean native SACs current) were rapidly inactivating ($\tau = 39.2 \pm 1.8$ ms, $n = 32$) and fast deactivating ($\tau = 10.7 \pm 0.6$ ms, $n = 32$; Fig 4C and supplementary Fig S4d online). Expression of PC2-WT or the PC2-740X mutant reduced Piezo1 activity in COS-7 cells, as previously observed in PCT cells (Fig 4C,D and Fig 5B). Importantly, when coexpressed with TRPC1, another TRP subunit, Piezo1 activity was not modified, thus demonstrating the specificity of the inhibitory effect observed with PC2-740X (Fig 4D). All together these findings indicate that PC2 regulates the stretch activation of Piezo1.

A possible mechanism for inhibition of SACs by PC2-740X might involve an effect on the biosynthesis and/or transporting of Piezo1 to the plasma membrane. However, confocal microscopy in PCT cells transfected with a Piezo1–enhanced green fluorescent protein (EGFP) construct revealed that Piezo1 localization at the plasma membrane (colocalization with WGA) was not altered by PC2-WT or PC2-740X expression (supplementary Figs S6 and S7 online). Thus, these findings indicate that transporting of Piezo1 to the plasma membrane is not modified by PC2 or PC2-740X expression. The stronger inhibition of SACs observed with the pathogenic mutant PC2-740X might be related either to higher PC2 mutant protein expression (5.3 ± 1.9 fold versus PC2, as determined by western blots, $n = 5$), increased targeting to the plasma membrane because of deletion of the endoplasmic reticulum retention signal and/or lack of interaction with PC1 because of deletion of the interacting coiled-coil domain [36,38].

Next, we investigated whether PC2 might interact, directly or indirectly, with Piezo1. Both MYC-tagged PC2-WT and PC2-740X coimmunoprecipitated with Piezo1-haemagglutinin in transiently transfected COS cells, unlike Kv2.1 or Kv9.3 (Fig 5A and supplementary Fig S8 online). The N-terminal domain of PC2 was critically required for the interaction and for inhibition of Piezo1 SAC activity (Fig 5A,B). Finally, when overexpressed in

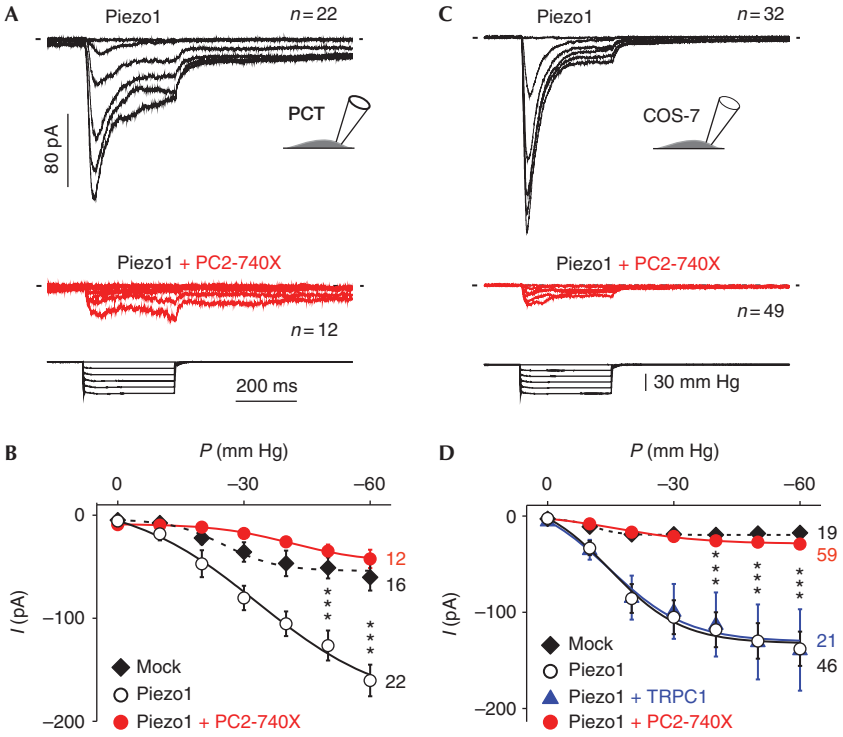

Fig 4 | Exogenous Piezo1 activity is conditioned by PC2-740X in PCT or COS-7-transfected cells. (**A**) The top trace in black shows the mean ($n = 22$) cell-attached SAC current at a holding potential of -80 mV in Piezo1 ires EGFP-transiently transfected PCT cells together with a DsRed mock vector. The middle trace in red shows the mean ($n = 12$) cell-attached SAC current at a holding potential of -80 mV in Piezo1 ires EGFP-transfected PCT cells together with PC2-740X ires2-DsRed. Bottom traces illustrate the pressure pulses. (**B**) Pressure-effect curves for SACs/Piezo1 activity (as indicated) in transfected PCT cells (control PCT cells transfected with a mixture of mock vectors EGFP and DsRed: $P_{0.5} = -25.3 \pm 2.0$ mm Hg, $k = 6.3 \pm 1.1$; Piezo1 ires EGFP + mock vector DsRed: $P_{0.5} = -32.7 \pm 4.2$ mm Hg, $k = 12.9 \pm 3.6$; Piezo1 ires EGFP + PC2-740X ires2-DsRed: $P_{0.5} = -41.1 \pm 1.6$ mm Hg, $k = 9.0 \pm 0.8$). *n*-values are indicated on the right side of the graph. (**C**) The top trace in black shows the mean ($n = 32$) cell-attached SAC current at a holding potential of -80 mV in Piezo1 ires EGFP-transfected COS-7 cells together with a mock vector DsRed. The middle trace in red shows the mean ($n = 49$) cell-attached SAC current at a holding potential of -80 mV in Piezo1 ires EGFP-transfected COS-7 cells together with PC2-740X ires2-DsRed. Bottom traces illustrate the pressure pulses. Same scales for **A** and **C**. (**D**) Pressure-effect curves for SACs/Piezo1 activity (as indicated) in transfected COS-7 cells (control COS cells transfected with a mixture of mock vectors EGFP and DsRed: $P_{0.5} = -10.9 \pm 1.5$ mm Hg, $k = 3.0 \pm 4.0$; Piezo1 ires EGFP + mock vector DsRed: $P_{0.5} = -14.9 \pm 1.5$ mm Hg, $k = 8.5 \pm 1.9$; Piezo1 ires EGFP + PC2-740X ires2-DsRed: $P_{0.5} = -16.9 \pm 1.2$ mm Hg, $k = 10.2 \pm 1.6$; Piezo1 ires EGFP + TRPC1 ires2-DsRed: $P_{0.5} = -14.6 \pm 2.1$ mm Hg, $k = 9.3 \pm 3.0$). *n*-values are indicated on the right side of the graph. In **A** and **C**, only patches in which the whole pressure range could be applied without rupture were included. EGFP, enhanced green fluorescent protein; PC2, Polycystin-2; PCT, proximal convoluted tubule; SAC, stretch-activated ion channel.

PCT cells, PC2-740X colocalized with Piezo1–EGFP at the plasma membrane (supplementary Fig S9 online).

In conclusion, we show that Piezo1 acts as a stretch-activated cationic channel in renal tubular epithelial cells and PC2, as well as its pathogenic mutants, inhibit its activity. We demonstrate a coimmunoprecipitation of PC2 together with Piezo1 in transfected cells, which is critically dependent on the N-terminal domain of PC2. These findings indicate that PC2 might interact via its N-terminal domain, either directly or indirectly, with Piezo1 thereby possibly inhibiting its stretch sensitivity at the plasma membrane. Overexpression of the PC2-740X mutant produced a large decrease in the amplitude of both native and exogenous Piezo1/SAC currents. The stronger effect on SACs observed with expression of PC2-740X might be related to the enhanced mutant protein expression, increased localization at the plasma membrane and/or a lack of interaction with PC1 [36]. This finding might illustrate the possible role of a dysregulated PC2/Piezo1 functional interaction in some aspects of PKD. We anticipate that our findings will provide a strong basis to further investigate the pathophysiological role of Piezo1 in kidney disease states associated with an increase in intrarenal pressure, including obstructive uropathies and PKD.

METHODS

Cell lines culture and transfection. COS-7 cells were cultured in DMEM (Gibco BRL Life Technologies) supplemented with 10% fetal calf serum (Hyclone). COS-7 were transfected using the DEAE-Dextran protocol. PCT cells were transfected using jetPEI (Polyplus transfection) according to the manufacturer's instructions. TRPC1, Piezo1 or the disease-causing mutant PC2-740X

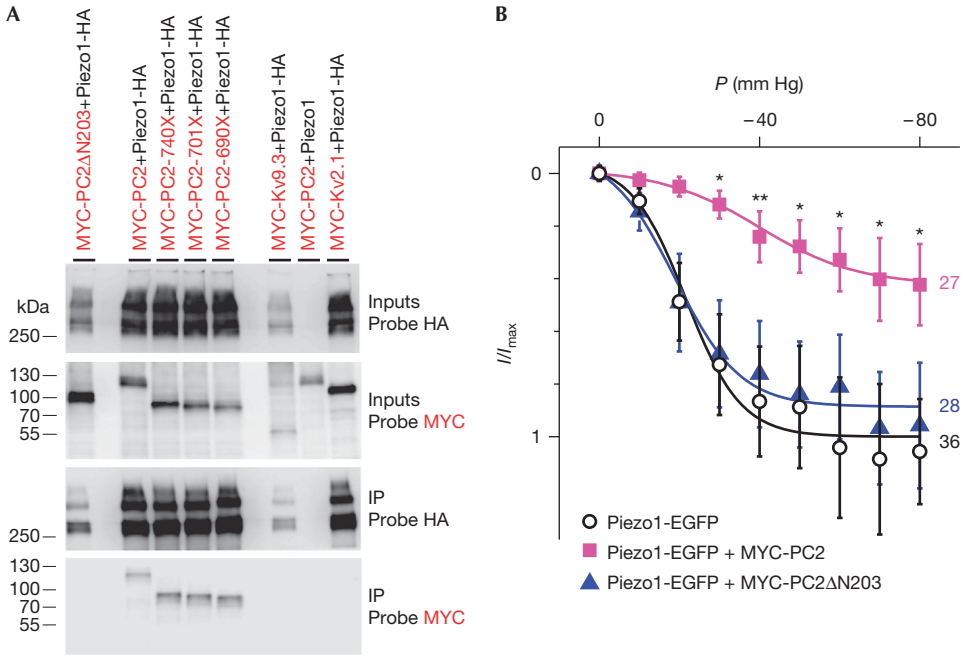

Fig 5 | PC2 and PC2 mutants coimmunoprecipitation with Piezo1 in transiently transfected COS cells. (**A**) Western blot analysis of lysates and immunoprecipitates from COS cells cotransfected with Piezo1-HA and either NH2 (ΔN203) or COOH terminal deletions (from −740X to −690X) in MYC-PC2 (as indicated) show that the NH2 terminus of PC2 is necessary for immunoprecipitation with Piezo1-HA, while the COOH terminus is not required (bottom most panel). Neither MYC-Kv2.1 nor MYC-Kv9.3 (used as negative controls) immunoprecipitate with Piezo-HA. Immunoprecipitation is absent without an HA tag on Piezo1. Blots were probed with 3F10 (Probe HA) or with 9E10 (Probe MYC). Inputs and IPs are as indicated. (**B**) Inhibition of Piezo1 by PC2 in cotransfected COS cells. Deletion of the N-terminal domain of PC2 (ΔN203) prevents Piezo1 inhibition (Piezo1-EGFP + mock vector DsRed: $P_{0.5} = -21.6 \pm 1.4$ mm Hg, $k = 6.8 \pm 1.2$; Piezo1-EGFP + MYC-PC2 ires2-DsRed: $P_{0.5} = -39.9 \pm 2.8$ mm Hg, $k = 12.2 \pm 2.2$; Piezo1-EGFP + MYC-PC2ΔN203 ires2-DsRed: $P_{0.5} = -18.9 \pm 1.5$ mm Hg, $k = 8.2 \pm 1.8$). All currents were normalized to the fitted value for Piezo1-EGFP + mock vector DsRed at −80 mm Hg. *n*-values are indicated on the right side of the graph. EGFP, enhanced green fluorescent protein; HA, haemagglutinin; SAC, stretch-activated ion channel; PC2, Polycystin-2; .

(inserted into ires2-EGFP or ires2-DsRed vectors) were transfected at 0.5 µg of plasmid DNA per 35-mm dish containing ~25,000 cells per dish.

Molecular biology, biochemistry and immunostainings. The mPC2 (Entrez GeneID: 5311) deletion construct (mPC2-740X), corresponding to the human pathogenic R742X mutant [39], was generated by PCR and cloned into a ires2-DsRed vector. TRPC1 coding sequences were cloned into a ires2-EGFP plasmid. EGFP as well as DsRed mock vectors were used in control experiments. All inserts were sequenced in their entirety. QPCR experiments were performed using Sybr green on a Light Cycler 480 (Roche). Oligonucleotide sequences are available on request. siRNAs directed against Piezo1 have been previously validated (initially called siRNA1 and siRNA3) in [25] and transfected in PCT cells using the HiPerFect Transfection Reagent (Qiagen SA, Courtaboeuf, France).

Electrophysiology. Electrophysiological procedure has been previously described elsewhere [24,32]. Briefly, single-channel cell-attached patch-clamp recordings were performed on isolated renal tubules (mean pipette resistance of 4.0 MΩ) or immortalized PCT and COS-7 cells (mean pipette resistance of 1.4 MΩ). The pipette medium contained (in mM): NaCl 150, KCl 5, $CaCl_2$ 2 and HEPES 10 (pH 7.4 with NaOH). The pipette solution also contained 10 mM TEA, 5 mM 4AP and 10 µM glibenclamide to inhibit eventual contaminating K^+ channels. The bath medium contained (in mM): KCl 155, EGTA 5, $MgCl_2$ 3 and HEPES 10 (pH 7.2 with KOH). The osmolarity of all solutions was adjusted to 310 mOsm. Membrane patches were stimulated with 300 ms long negative pressure pulses of −10 mm Hg increments with a period of 3 s, through the recording electrode using a fast pressure-clamp device (ALA High Speed Pressure Clamp-1 System, ALA-Scientific). The holding voltage for all experiments was −80 mV for SACs recordings, unless otherwise indicated. Detailed information about materials and methods is available in the Supplementary Information online. Statistical significance: $^*P<0.05$; $^{**}P<0.01$; $^{***}P<0.001$.

Supplementary information is available at EMBO *reports* online (http://www.emboreports.org).

ACKNOWLEDGEMENTS
We are grateful to the ANR 2008 ''Du gène à la physiopathologie; des maladies rares aux maladies communes'' and ANR 2011 ''Physiologie, physiopathologie, santé publique'', to the Fondation de la recherche médicale, to the Fondation de recherche sur l'hypertension artérielle, to the Fondation de France, to the Association Française contre les Myopathies (RP), to the Association pour l'information et la recherche sur les maladies rénales génétiques France, to the Région Provence Alpes Côte d'Azur, to the Société Française d'hypertension artérielle, to the Université de Nice Sophia Antipolis and to Centre National de la

Recherche Scientifique for financial support. We thank L. Tsokias for providing the mouse *Pkd2* plasmid, A. Patapoutian for the gift of the Piezo1 ires EGFP plasmid and F. Sachs and T. Suchyna for the gift of GsMTx-4.

Author contributions: R.P. and J.R.M. did the patch-clamp experiments. F.D., S.D., M.T., C.D., M.P. and J.T. helped with renal PCT cells isolation, as well as electrophysiological recordings on isolated renal tubules. A.P. generated the molecular biology reagents and performed the biochemistry experiments. M.J. was in charge of cell culture and M.A. carried out the QPCR experiments. E.H. supervised the research, performed experiments and wrote the manuscript together with A.P.

CONFLICT OF INTEREST

The authors declare that they have no conflict of interest.

REFERENCES

1. Chalfie M (2009) Neurosensory mechanotransduction. *Nat Rev Mol Cell Biol* **10:** 44–452
2. Kung C (2005) A possible unifying principle for mechanosensation. *Nature* **436:** 647–654
3. Gillespie PG, Walker RG (2001) Molecular basis of mechanosensory transduction. *Nature* **413:** 194–202
4. Nilius B, Honore E (2012) Sensing pressure with ion channels. *Trends Neurosci* **35:** 477–486
5. Delmas P, Hao J, Rodat-Despoix L (2011) Molecular mechanisms of mechanotransduction in mammalian sensory neurons. *Nat Rev Neurosci* **12:** 139–153
6. Wood JN, Eijkelkamp N (2012) Noxious mechanosensation–molecules and circuits. *Curr Opin Pharmacol* **12:** 4–8
7. Smith ES, Lewin GR (2009) Nociceptors: a phylogenetic view. *J Comp Physiol A Neuroethol Sens Neural Behav Physiol* **195:** 1089–1106
8. Sachs F, Morris CE (1998) Mechanosensitive ion channels in nonspecialized cells. *Rev Physiol Biochem Pharmacol* **132:** 1–77
9. Nauli SM *et al* (2003) Polycystins 1 and 2 mediate mechanosensation in the primary cilium of kidney cells. *Nat Genet* **33:** 129–137
10. Praetorius HA, Spring KR (2003) The renal cell primary cilium functions as a flow sensor. *Curr Opin Nephrol Hypertens* **12:** 517–520
11. Patel A, Honore E (2010) Polycystins and renovascular mechanosensory transduction. *Nat Rev Nephrol* **6:** 530–538
12. Delmas P (2004) Polycystins: from mechanosensation to gene regulation. *Cell* **118:** 145–148
13. Weinbaum S, Duan Y, Satlin LM, Wang T, Weinstein AM (2010) Mechanotransduction in the renal tubule. *Am J Physiol Renal Physiol* **299:** F1220–F1236
14. Nauli SM, Zhou J (2004) Polycystins and mechanosensation in renal and nodal cilia. *Bioessays* **26:** 844–856
15. Jensen ME, Odgaard E, Christensen MH, Praetorius HA, Leipziger J (2007) Flow-induced [Ca2 +]i increase depends on nucleotide release and subsequent purinergic signaling in the intact nephron. *J Am Soc Nephrol* **18:** 2062–2070
16. Quinlan MR, Docherty NG, Watson RW, Fitzpatrick JM (2008) Exploring mechanisms involved in renal tubular sensing of mechanical stretch following ureteric obstruction. *Am J Physiol Renal Physiol* **295:** F1–F11
17. Rohatgi R, Flores D (2010) Intratubular hydrodynamic forces influence tubulointerstitial fibrosis in the kidney. *Curr Opin Nephrol Hypertens* **19:** 65–71
18. Wyker AT, Ritter RC, Marion D, Gillenwater JY (1981) Mechanical factors and tissue stresses in chronic hydronephrosis. *Invest Urol* **18:** 430–436
19. Power RE, Doyle BT, Higgins D, Brady HR, Fitzpatrick JM, Watson RW (2004) Mechanical deformation induced apoptosis in human proximal renal tubular epithelial cells is caspase dependent. *J Urol* **171:** 457–461
20. Cachat F, Lange-Sperandio B, Chang AY, Kiley SC, Thornhill BA, Forbes MS, Chevalier RL (2003) Ureteral obstruction in neonatal mice elicits segment-specific tubular cell responses leading to nephron loss. *Kidney Int* **63:** 564–575
21. Praetorius HA, Frokiaer J, Leipziger J (2009) Transepithelial pressure pulses induce nucleotide release in polarized MDCK cells. *Am J Physiol Renal Physiol* **288:** 133–141
22. Derezic D, Cecuk L (1982) Hydrostatic pressure within renal cysts. *Br J Urol* **54:** 93–94
23. Tanner GA, McQuillan PF, Maxwell MR, Keck JK, McAteer JA (1995) An *in vitro* test of the cell stretch-proliferation hypothesis of renal cyst enlargement. *J Am Soc Nephrol* **6:** 1230–1241
24. Peyronnet R *et al* (2012) Mechanoprotection by polycystins against apoptosis is mediated through the opening of stretch-activated K(2P) channels. *Cell Rep* **1:** 241–250
25. Coste B, Mathur J, Schmidt M, Earley TJ, Ranade S, Petrus MJ, Dubin AE, Patapoutian A (2010) Piezo1 and Piezo2 are essential components of distinct mechanically activated cation channels. *Science* **330:** 55–60
26. Coste B *et al* (2012) Piezo proteins are pore-forming subunits of mechanically activated channels. *Nature* **483:** 176–181
27. Kim SE, Coste B, Chadha A, Cook B, Patapoutian A (2012) The role of *Drosophila* Piezo in mechanical nociception. *Nature* **483:** 209–212
28. Coste B *et al* (2013) Gain-of-function mutations in the mechanically activated ion channel PIEZO2 cause a subtype of distal arthrogryposis. *Proc Natl Acad Sci USA* **110:** 4667–4672
29. Zarychanski R, Schulz VP, Houston BL, Maksimova Y, Houston DS, Smith B, Rinehart J, Gallagher PG (2012) Mutations in the mechanotransduction protein PIEZO1 are associated with hereditary xerocytosis. *Blood* **120:** 1908–1915
30. Bae C, Gnanasambandam R, Nicolai C, Sachs F, Gottlieb PA (2013) Xerocytosis is caused by mutations that alter the kinetics of the mechanosensitive channel PIEZO1. *Proc Natl Acad Sci USA* **110:** E1162–E1168
31. IAndolfo I *et al* (2013) Multiple clinical forms of dehydrated hereditary stomatocytosis arise from mutations in PIEZO1. *Blood* **121:** 3925–3935
32. Sharif Naeini R *et al* (2009) Polycystin-1 and -2 dosage regulates pressure sensing. *Cell* **139:** 587–596
33. Burtey S, Riera M, Ribe E, Pennekamp P, Passage E, Rance R, Dworniczak B, Fontes M (2008) Overexpression of PKD2 in the mouse is associated with renal tubulopathy. *Nephrol Dial Transplant* **23:** 1157–1165
34. Gallagher AR *et al* (2006) A truncated polycystin-2 protein causes polycystic kidney disease and retinal degeneration in transgenic rats. *J Am Soc Nephrol* **17:** 2719–2730
35. Park EY *et al* (2008) CYST formation kidney *via* B-RAF signaling in the PKD2 transgenic mice. *J Biol Chem* **284:** 7214–7222
36. Chen XZ *et al* (2001) Transport function of the naturally occurring pathogenic polycystin-2 mutant, R742X. *Biochem Biophys Res Commun* **282:** 1251–1256
37. Thivierge C, Kurbegovic A, Couillard M, Guillaume R, Cote O, Trudel M (2006) Overexpression of PKD1 causes polycystic kidney disease. *Mol Cell Biol* **26:** 1538–1548
38. Tsiokas L, Kim E, Arnould T, Sukhatme VP, Walz G (1997) Homo- and heterodimeric interactions between the gene products of PKD1 and PKD2. *Proc Natl Acad Sci USA* **94:** 6965–6970
39. Qian F, Germino FJ, Cai Y, Zhang X, Somlo S, Germino GG (1997) PKD1 interacts with PKD2 through a probable coiled-coil domain. *Nat Genet* **16:** 179–183
40. Suchyna TM, Tape SE, Koeppe RE 2nd, Andersen OS, Sachs F, Gottlieb PA (2004) Bilayer-dependent inhibition of mechanosensitive channels by neuroactive peptide enantiomers. *Nature* **430:** 235–240